

# Experimental study of relationship between interfacial electroadhesive force and applied voltage for different substrate materials

J. Guo, T. Bamber, J. Petzing, L. Justham, and M. Jackson

Citation: *Appl. Phys. Lett.* **110**, 051602 (2017); doi: 10.1063/1.4975602

View online: <http://dx.doi.org/10.1063/1.4975602>

View Table of Contents: <http://aip.scitation.org/toc/apl/110/5>

Published by the [American Institute of Physics](#)

---

## Articles you may be interested in

[Ultrafast photocurrent measurements of a black phosphorus photodetector](#)

*Appl. Phys. Lett.* **110**, 051102051102 (2017); 10.1063/1.4975360

[Strong coupling between Tamm plasmon polariton and two dimensional semiconductor excitons](#)

*Appl. Phys. Lett.* **110**, 051101051101 (2017); 10.1063/1.4974901

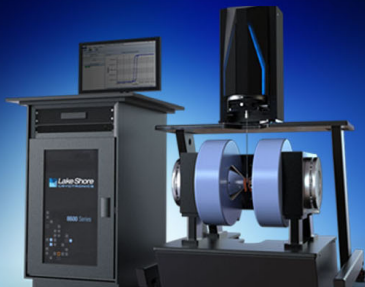
[Nontrivial surface state transport in Bi<sub>2</sub>Se<sub>3</sub> topological insulator nanoribbons](#)

*Appl. Phys. Lett.* **110**, 053108053108 (2017); 10.1063/1.4975386

[Water-driven actuation of \*Ornithoctonus huwena\* spider silk fibers](#)


*Appl. Phys. Lett.* **110**, 053103053103 (2017); 10.1063/1.4974350

---



## NEW 8600 Series VSM

For fast, highly sensitive measurement performance

LEARN MORE 

## Experimental study of relationship between interfacial electroadhesive force and applied voltage for different substrate materials

J. Guo,<sup>a)</sup> T. Bamber, J. Petzing, L. Justham, and M. Jackson

*The Wolfson School of Mechanical, Electrical and Manufacturing Engineering, Loughborough University, Loughborough, Leicestershire LE11 3TU, United Kingdom*

(Received 20 December 2016; accepted 23 January 2017; published online 1 February 2017)

An experimental investigation into the relationship between the interfacial electroadhesive force and applied voltage up to 20 kV has been presented. Normal electroadhesive forces have been obtained between a double-electrode electroadhesive pad and three optically flat and different substrate materials: glass, acrylic, and polycarbonate. The results have shown that not all substrate materials are good for the generation of electroadhesive forces. Only 15.7 Pa has been obtained between the pad and the polycarbonate substrate under 20 kV, whereas 46.3 Pa and 123.4 Pa have been obtained on the acrylic and glass substrate, respectively. Based on the experimental data, empirical models, with an adjusted R-square value above 0.995 in all cases, have been obtained for the three substrates. However, it has not been possible to develop a general empirical model which is suitable for all substrates. This further indicates the need for a large quantity of experimental data to obtain robust empirical models for different substrate materials in order to reliably use electroadhesive technologies for material handling applications. © 2017 Author(s). All article content, except where otherwise noted, is licensed under a Creative Commons Attribution (CC BY) license (<http://creativecommons.org/licenses/by/4.0/>). [<http://dx.doi.org/10.1063/1.4975602>]

Electroadhesion<sup>1</sup> is an electrically controllable adhesion phenomenon between two interfacial surfaces: an energized electroadhesive pad and a substrate, subjected to strong electric fields. The electroadhesive pad is made of conductive electrodes connected with high voltage power sources, usually in the range of kilovolts (kV), and embedded in a dielectric material. The substrate is the material to which the electroadhesion, induced by either high voltage polarization or electric induction,<sup>2</sup> is applied, including walls to hold onto or objects to be picked up. Compared to other adhesion mechanisms,<sup>3</sup> this advanced adhesion mechanism has several advantages including enhanced adaptability, reduced complexity, decreased energy consumption, quiet in operation, and flexibility and non-damaging interactions for material handling applications.<sup>4</sup> As such, the electroadhesion technology has been used by the researchers investigating mobile robots including climbing<sup>5</sup> and perching<sup>6</sup> robots and in end effectors for robotic material handling applications.<sup>4,7,8</sup>

Electroadhesion is a dynamic electrostatic attraction phenomenon with over 33 variables influencing the interfacial electroadhesive forces obtainable between the two surfaces,<sup>9</sup> among which the applied voltage magnitude is one of the most dominating factors. The previous theoretical and simulation results have shown that the interfacial electroadhesive force is proportional to the square of the applied voltage.<sup>10,11</sup> The experiment results, especially the results from the recent work by Koh *et al.*,<sup>12</sup> however, have consistently demonstrated the inappropriateness of this pure quadratic relationship.<sup>12–15</sup> Also, there is a lack of a standardised or recognised experiment setup and procedure to investigate this relationship, especially by taking the surface texture of

the interfacial surfaces and environmental factors into consideration.<sup>9</sup> This is because the interfacial electroadhesive forces can be greatly influenced by surface scratches<sup>9</sup> and changing environmental factors such as humidity and temperature.<sup>2</sup> In addition, little work has been published previously regarding the relationship between the interfacial electroadhesive force achieved and applied voltage up to 20 kV. Furthermore, there is a lack of specific empirical models describing the relationship between the force and voltage magnitude on different substrate materials.

This paper begins with an introduction to an in-house electroadhesive pad design and manufacture process. After this, a repeatable electroadhesive force measurement procedure, performed in a controlled and mechatronic force measurement platform, is presented. Surface texture measurement and characterisation of the three substrates and the pad surfaces are then conducted using a Zygo and the Talymap surface texture data analysis software. Followed by this, the electroadhesive force measurement is performed and empirical models are derived based on the experimental data. Discussion and conclusions are finally made based on the achieved results.

The electroadhesive pad design and manufacturing process was based on solid-ink printing, chemical etching, and conformal coating.<sup>16</sup> The electrode geometry design was conducted in SOLIDWORKS and based on a double-electrode design, where one electrode was connected to a positive high voltage source and the other one was connected to a negative high voltage source. As can be seen in Fig. 1, the effective electrode area was set as 190 mm × 190 mm. Please note that the width and length of the electrodes can be other values for this investigation. Also, dielectric breakdown will occur if small gaps are adopted. The space between the electrodes was set as 20 mm to endure high

<sup>a)</sup> Author to whom correspondence should be addressed. Electronic mail: J.Guo@lboro.ac.uk

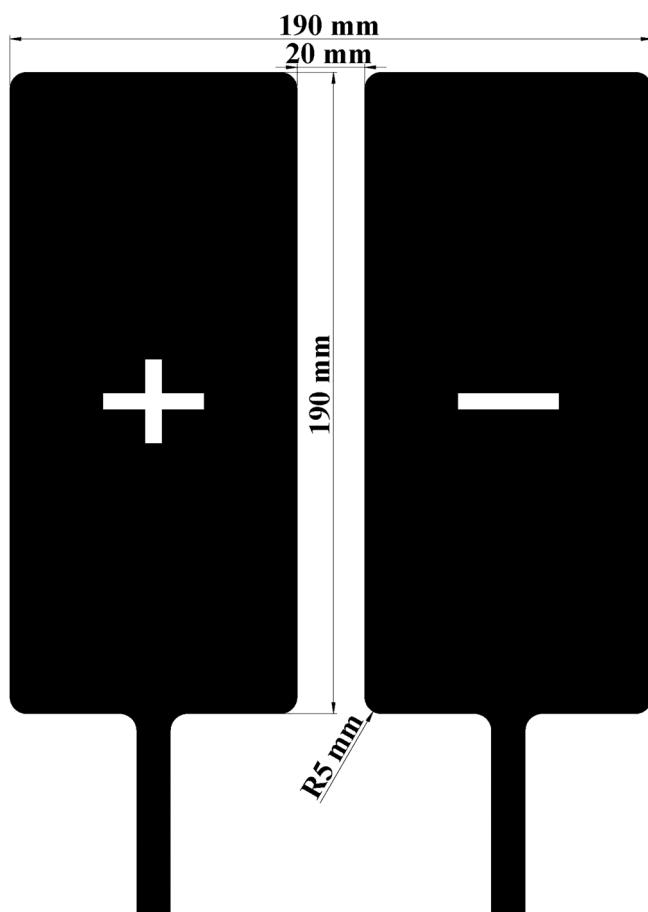


FIG. 1. Electrode geometric design and dimensions.

voltages up to 20 kV. The corners of the electrodes were rounded to decrease the charge concentration problem.

The electrode design was then printed onto a cleaned 297 mm × 210 mm size copper laminate (GTS Flexible Materials Limited, UK) via a Xerox solid-ink printer. The copper laminate comprises a 35 μm thick copper adhered onto a 75 μm thick polyester (PET). The wax protected copper laminate was then placed into a pre-heated bubble etching tank (Mega Electronics, UK) filled with ferric chloride granules (2000 g, RS Components, UK) mixed with 4-liter water. The unwanted copper areas were completely etched within 5 min. The etched copper laminate was removed from the etching tank, and the remaining wax was removed using a label removal spray (Farnell, UK) and cleaned via an Isopropyl Alcohol (Farnell, UK) in a spray booth. After this, aerosol conformal coating of a polyurethane (PUC, RS Components, UK) was conducted on the completely cleaned and dried copper laminate. An ultraviolet light pen was used to ensure an even coating before vacuum degassing and 90 min's curing of the pad in a vacuum oven (Fistreem International Ltd., UK) at 80° was undertaken.

A mechatronic and reconfigurable force measurement platform has been designed and used to obtain the normal electroadhesive forces between the electroadhesive pad and substrate.<sup>9</sup> As aforementioned, unstable forces have been achieved when testing the pads in ambient environments. A custom built environmental chamber has been developed to maintain the temperature and humidity.<sup>2</sup> The chamber was made of an insulating foam and controlled by an air

conditioning unit and a dehumidifier. A repeatable electroadhesive force measurement procedure, as can be seen in Fig. 2, has been used.

The pad was initially attached on a pad holder and the substrates. The pad was driven down towards the substrate by a servo motor (driven by a Kollmorgen motor driver connected with a CompactRio) until a  $22 \pm 0.5$  N preload was applied between the pad and substrate. The pad was then energized by two high voltage converters (HVCs, EMCO High Voltage Corporation), with ( $\pm$ ) 0–10 kV output and 0–5 V reference input, which was from an Instek GPD 3303 direct current power supply unit (DC PSU, GW Instek). A 6-axis force/torque (F/T) sensor (ATI Industrial Automation, UK), with a tolerance of  $\pm 0.05$  N, was employed to record the forces. The recording of the normal electroadhesive force was thus started after turning on the DC PSU. The pad was charged for 60 s before pulling the pad away from the substrate using a velocity of  $0.1 \text{ mms}^{-1}$  and an acceleration of  $50 \text{ revs}^{-2}$ . As can be seen from Fig. 2, during the pulling-off phase, the electroadhesive force decreases as the gap increases between the pad and substrate. The PSU was then turned off after 15 s.

Due to the residual charge on the pad, the electroadhesive force does not drop immediately but it decreases gradually. The force data recording were stopped when the force reached zero, and the data were exported as text files. These files were loaded and further analyzed in MATLAB. 520 s' dwell time was used for the residual charge dissipation, and both the pad and the substrates were grounded for 300 seconds after each test during this period. An electrostatic fieldmeter (Simco-Ion) was used to measure the surface charge of the pad and substrates. 300 s was enough to obtain repeatable results for this study. A fixed experiment time of 10 min for each test was, therefore, set. For each substrate, five experiments were repeated. The average of the five results and its standard deviation were reported.

As aforementioned, the direction of the surface texture of the substrate surface plays an important role in achieving

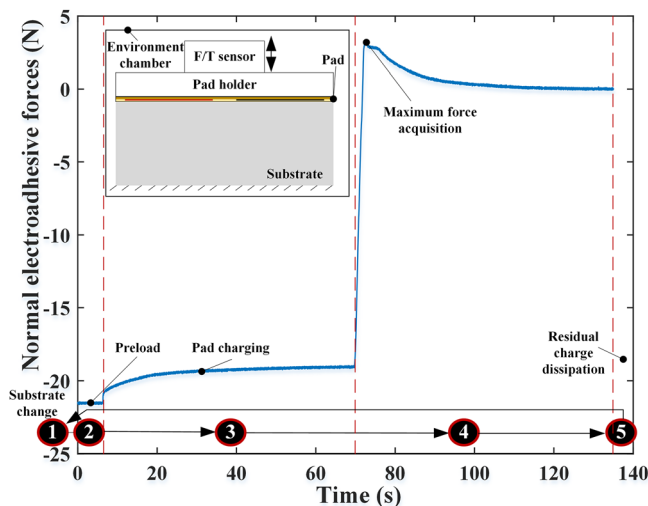


FIG. 2. Electroadhesive force measurement procedure, where five steps are employed: (1) change substrates, (2) record the force and set the preload, (3) charge the pad, (4) pull away the pad holder to obtain the maximum electroadhesive force, and (5) discharge the pad and substrate.

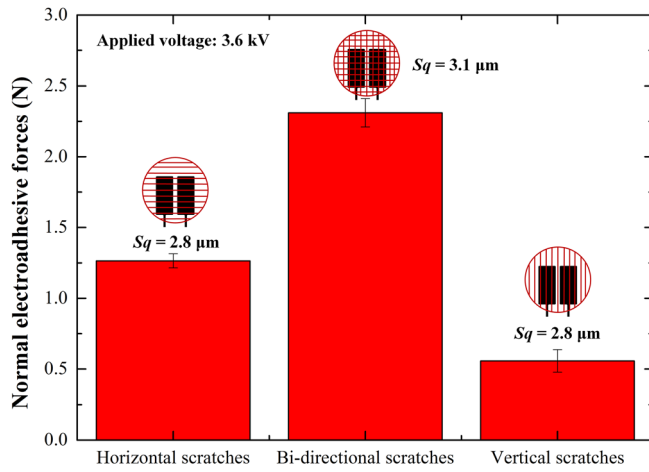


FIG. 3. Normal electroadhesive forces obtained between the pad and Al plates with different surface scratches.

a repeatable and controllable electroadhesive force. The electroadhesive force obtained from the double-electrode pad produced in this study is also sensitive to different surface scratches, as shown in Fig. 3. Three sanded aluminium (Al) plates with horizontal (the root mean square height,  $Sq = 2.8 \mu\text{m}$ ), bi-directional ( $Sq = 2.8 \mu\text{m}$ ), and vertical scratches ( $Sq = 2.8 \mu\text{m}$ )<sup>9</sup> have been used as the substrates to investigate the relationship between the interfacial electroadhesive force and different surface scratches. The same experimental setup and procedure, as described in the last section, have been used. The pad was charged at 3.6 kV. Please note that the substrate change order was Al substrate with horizontal scratches, Al substrate with bi-directional scratches, and Al substrate with vertical scratches. Different forces were obtained on the three different surface scratches. As demonstrated in Fig. 3, a relative difference of 312.5% in forces obtainable can be seen between the results on the Al plate with bi-directional scratches (2.31 N) and vertical scratches (0.56 N).

In order to investigate the influence of different substrate materials, it is therefore important to prepare substrate materials with similar surface textures. A toughened glass plate, an acrylic plate, and a polycarbonate plate, with optically flat surface texture and the same dimensions (400 mm × 500 mm × 12 mm), were chosen as the substrate materials. Ten random areas from each substrate surfaces were measured by a Zygo NewView 5000, which is a non-contact surface texture measurement platform, with a Mirau 10× objective. The raw data from the Zygo software were analyzed in the Talymap commercial surface texture data analysis software. One typical form-removed surface texture information from the three substrate surfaces and the PET side of the pad can be seen in Fig. 4.

A standard Gaussian filter with a cut-off length of 0.25 mm was applied, and end effects were managed using the Talymap software. The  $Sq$  of the acrylic, glass, polycarbonate, and PET surface is 3.2 nm, 2.4 nm, 1.7 nm, and 37.2 nm, respectively. The average of the  $Sq$  values of ten random areas on each substrate surface and their standard deviations are plotted in Fig. 4(e).

The electroadhesive forces change when tested in different environment conditions. The results shown in Fig. 5,

obtained in two different environment conditions, clearly support this finding. The electroadhesive forces obtained when the relative humidity was maintained at  $49 \pm 1\%$ , room temperature at  $21.1 \pm 0.2^\circ\text{C}$ , and pressure at  $1008 \pm 0.2 \text{ hPa}$  were higher than the forces obtained when the relative humidity was maintained at  $39 \pm 1\%$ , room temperature at  $20.9 \pm 0.1^\circ\text{C}$ , and pressure at  $1013.5 \pm 0.1 \text{ hPa}$ . In order to compare the forces obtainable on the three different substrate materials at different voltage levels, the experiments were conducted when the relative humidity was maintained at  $49 \pm 1\%$ , room temperature at  $21.1 \pm 0.2^\circ\text{C}$ , and pressure at  $1008 \pm 0.2 \text{ hPa}$ .

A voltage difference up to 20 kV, in the steps of 1.2 kV, was applied on the pad. Different experiment results were obtained on the three substrates, as demonstrated in Figs. 6–8. For the electroadhesive forces obtained on the acrylic substrate, as presented in Fig. 6, the empirical model of Equation (1) was derived

$$F = 0.06 - 0.00124U - 0.00037U^2 + 0.00081U^3 + 0.00003U^4, \quad (1)$$

where  $F$  denotes the normal electroadhesive force and  $U$  denotes the applied voltage.

For the electroadhesive forces obtained on the polycarbonate substrate, as presented in Fig. 7, the empirical model was derived as

$$F = 0.21 + 0.003U + 0.00073U^2. \quad (2)$$

For the electroadhesive forces obtained on the glass substrate, as presented in Fig. 8, the empirical model was derived as

$$F = 5.54 + \frac{5.5}{1 + \left(\frac{U}{7.11}\right)^{2.44}}. \quad (3)$$

The adjusted R-square values between the experimental data and the empirical models are all above 0.995. It has to be noted, however, that the general force increase trend does not change when the environment changes, as shown in Fig. 5. The empirical model for the forces obtained in  $39 \pm 1\%$ ,  $20.9 \pm 0.1^\circ\text{C}$ , and  $1013.5 \pm 0.1 \text{ hPa}$  was derived as

$$F = 4.69 - \frac{4.63}{1 + \left(\frac{U}{7.81}\right)^{2.84}}. \quad (4)$$

Up to now, there is no clear relationship between the electroadhesive force obtainable and the individual humidity or temperature or pressure. This is because it is difficult to control the humidity, temperature, and pressure independently. Future work on this is thus required. For the glass substrate, however, it has been found out that humidity has a greater influence on the forces than temperature and pressure. This is because that the glass substrate's dielectric property is sensitive to humidity change.

It is clear in the Figs. 6–8 that different substrate materials exhibit different electroadhesion properties. As can be

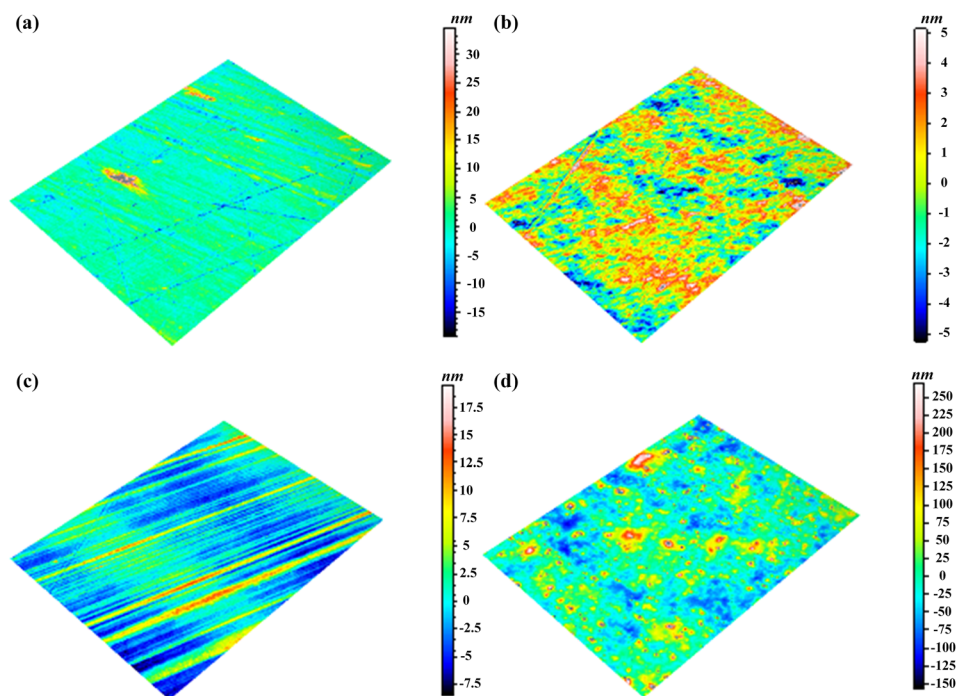


FIG. 4. Surface texture information of one typical area of the three substrates and the pad surface, where (a) is from the acrylic surface, (b) is from the polycarbonate surface, (c) is from the glass surface, (d) is from the PET surface, and (e) is the mean  $Sq$  values of the three substrate and pad surfaces.

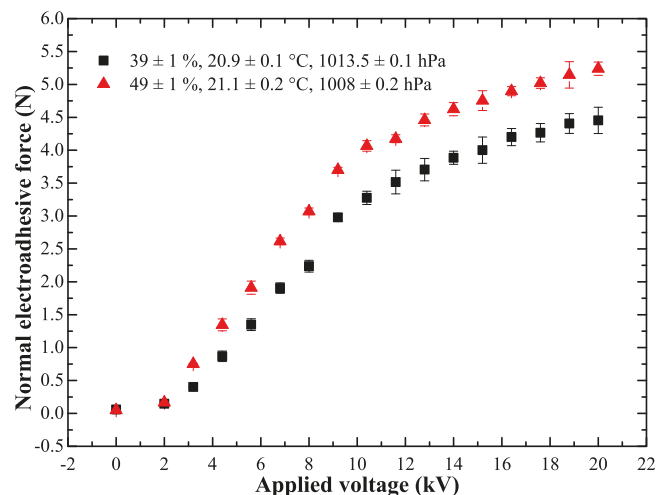
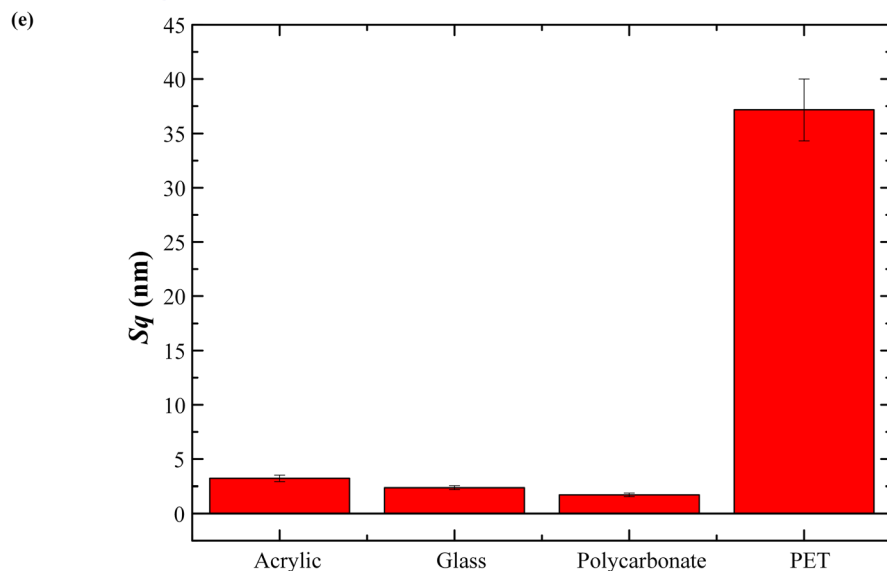


FIG. 5. Electroadhesive forces on the glass substrate obtained in different environments.

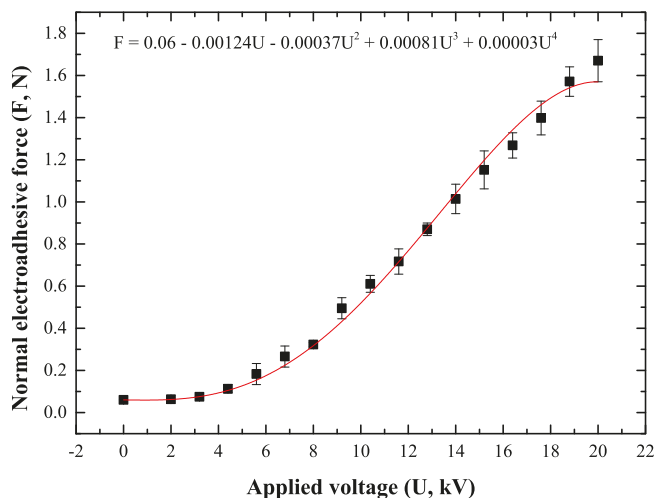


FIG. 6. Empirical model for the electroadhesive forces on the acrylic substrate.

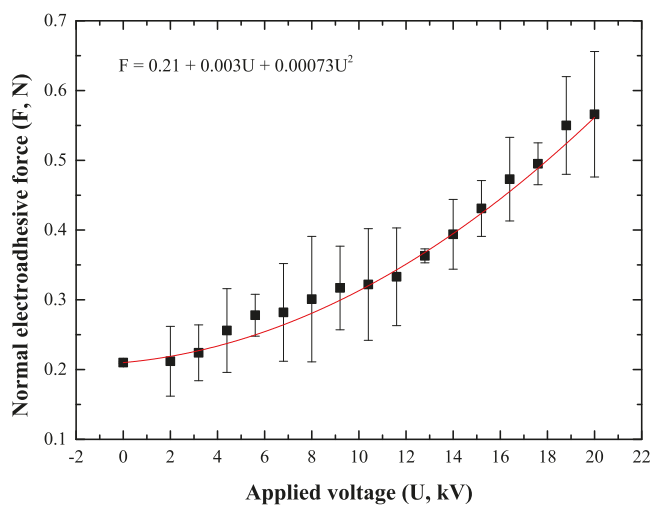


FIG. 7. Empirical model for the electroadhesive forces on the polycarbonate substrate.

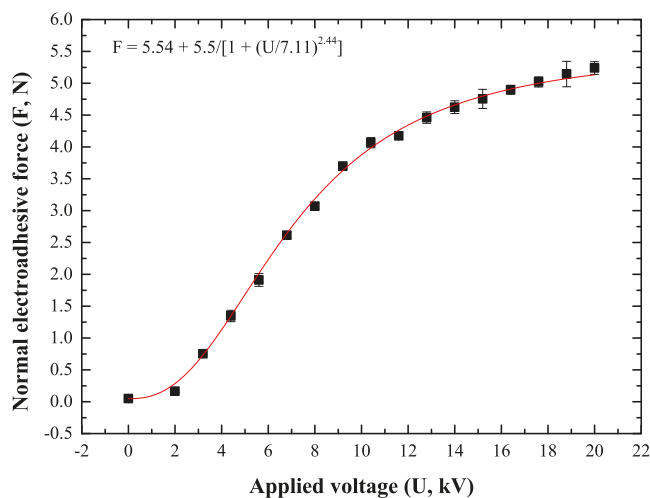


FIG. 8. Empirical model for the electroadhesive forces on the glass substrate.

seen from Fig. 7, the polycarbonate substrate exhibited poor electroadhesion characteristics compared to glass and acrylic. This means that not all substrate materials are appropriate for electroadhesive material handling applications. In addition, it can be concluded that there is no clear relationship between the electroadhesive forces obtained after charging 60 seconds and dielectric constants.

For the acrylic substrate, within the 20 kV range measured, the relationship between the interfacial electroadhesive force and applied voltage is polynomial or power. The adjusted R-square values of a parabola, cubic, quartic, allometric2 fit (default functions from Origin 9) were 0.979, 0.979, 0.997, and 0.969, respectively. The quartic fit was therefore selected as the empirical relationship. For the polycarbonate substrate, within the 20 kV range measured, the relationship between the interfacial electroadhesive force and applied voltage is also polynomial. The adjusted R-square values of a parabola, cubic, and quartic fit were all 0.997. For the glass substrate, within the 20 kV range measured, the relationship between the interfacial electroadhesive force and applied voltage can be polynomial. A logistics fit can also bring a good fit. In addition, a combination of

polynomial when the applied voltage is less than 6.8 kV and exponential when the applied voltage is beyond 6.8 kV can also produce a good fit. The adjusted R-square values of a quartic, combination of parabola and expdec1, langmuirext1, and logistics fit (default functions from Origin 9) were 0.9978, 0.98, 0.998, and 0.9983, respectively. The results have shown that there is no general empirical model that can be applied to all substrate materials.

Although the adjusted R-square values between the experimental data and the empirical models were all above 0.969, there is still a slight disagreement between the empirical model and the experimental results. This is due to the fact that the output of the HVC is not exactly linear with the reference input. There is an output tolerance of within +5% for the positive HVC and -10% for negative HVC.

Three different empirical models, with the goodness-of-fit above 0.995, in all cases, for the relationship between the interfacial electroadhesive force and applied voltage up to 20 kV, have been obtained for glass ( $Sq$ : 2.4 nm), acrylic ( $Sq$ : 3.2 nm), and polycarbonate ( $Sq$ : 1.7 nm) substrates with optically flat surface texture and the same geometric dimensions (400 mm  $\times$  500 mm  $\times$  12 mm). The results have shown that: different substrate materials exhibit different electroadhesion properties; not all substrate materials are good for electroadhesive material handling applications; and there is no general empirical model that can be applied to all substrate materials. A large number of further experiments are therefore needed to obtain robust empirical models for different substrate materials for future electroadhesive material handling applications.

The authors acknowledge the support from the EPSRC Centre for Innovative Manufacturing in Intelligent Automation in undertaking this research work under Grant Reference No. EP/IO33467/1.

<sup>1</sup>K. Rahbek, "Electroadhesion apparatus," U.S. patent 2,025,123 (24 December 1935).

<sup>2</sup>J. Guo, T. Bamber, M. Chamberlain, L. Justham, and M. Jackson, *J. Phys. D: Appl. Phys.* **49**(41), 415304 (2016).

<sup>3</sup>J. Guo, L. Justham, M. Jackson, and R. Parkin, *Key Eng. Mater.* **649**, 22–29 (2015).

<sup>4</sup>See <http://grabitinc.com/> for information about the advantages and applications of electroadhesion; accessed 2 December 2016.

<sup>5</sup>R. Liu, R. Chen, H. Shen, and R. Zhang, *Int. J. Adv. Rob. Syst.* **10**(36), 1–9 (2012).

<sup>6</sup>M. Graule, P. Chirattananon, S. Fuller, N. Jafferis, K. Ma, M. Spenko, R. Kornbluh, and R. Wood, *Science* **352**, 978–982 (2016).

<sup>7</sup>Z. Zhang, *IEEE/ASME Trans. Mechatronics* **4**(1), 39–49 (1999).

<sup>8</sup>G. J. Monkman, *Int. J. Rob. Res.* **14**(2), 144–151 (1995).

<sup>9</sup>J. Guo, M. Taylor, T. Bamber, M. Chamberlain, L. Justham, and M. Jackson, *J. Phys. D: Appl. Phys.* **49**(3), 35303 (2016).

<sup>10</sup>J. Mao, L. Qin, W. Zhang, L. Xie, and Y. Wang, *Eur. Phys. J. Appl. Phys.* **69**, 11003 (2015).

<sup>11</sup>C. Cao, X. Sun, Y. Fang, Q. Qin, A. Yu, and X. Feng, *Mater. Des.* **89**, 485–491 (2016).

<sup>12</sup>K. H. Koh, M. Sreekumar, and S. G. Ponnambalam, *Materials* **7**, 4963–4981 (2014).

<sup>13</sup>K. Asano, F. Hatakeyama, and K. Yatsuzuka, *IEEE Trans. Ind. Appl.* **38**, 840–845 (2002).

<sup>14</sup>J. Krahn and C. Menon, *Langmuir* **28**(12), 5438–5443 (2012).

<sup>15</sup>J. Guo, "Numerical and experimental study of electroadhesion to enable manufacturing automation," Ph.D. thesis (Loughborough University, 2016).

<sup>16</sup>J. Guo, T. Bamber, T. Hovell, M. Chamberlain, L. Justham, and M. Jackson, *IFAC-PapersOnLine* **49**(21), 309–315 (2016).